

# We are IntechOpen, the world's leading publisher of Open Access books Built by scientists, for scientists

6,900

Open access books available

185,000

International authors and editors

200M

Downloads

Our authors are among the

154

Countries delivered to

TOP 1%

most cited scientists

12.2%

Contributors from top 500 universities



WEB OF SCIENCE™

Selection of our books indexed in the Book Citation Index  
in Web of Science™ Core Collection (BKCI)

Interested in publishing with us?  
Contact [book.department@intechopen.com](mailto:book.department@intechopen.com)

Numbers displayed above are based on latest data collected.  
For more information visit [www.intechopen.com](http://www.intechopen.com)



# Single-Cell Transcriptome Analysis in Tumor Tissues

*Sadahiro Iwabuchi and Shinichi Hashimoto*

## Abstract

The tumor microenvironment is comprised of cancer cells and their surroundings, including various normal cells and non-cellular components, and each tumor tissue has a distinctive microenvironment. Cancer progression is affected by different microenvironmental states, such as the heterogeneity of infiltrating immune cells. Therefore, it is necessary to understand the complex cell-to-cell interactions associated with tumor developmental stages in different tissues. Recent revolution of single-cell RNA sequencing technology can uncover the tumor microenvironment diversity. We have developed a novel strategy of single-cell transcriptome analysis: next generation 1-cell sequencing (Nx1-seq) technology, and it allows for profiling of thousands of single cells from tumor tissue. Our microwell with cell bar-code beads device can detect genes with high sensitivity, and it is easily transported anywhere without any other dedicated devices. Further, the developmental cost is relatively cheaper than other single-cell RNA sequencing methods. In this study, we introduce representative application of the single-cell RNA sequencing technique in gynecological cancers, and we show the result of Nx1-seq application in human endometrioid adenocarcinoma tissue.

**Keywords:** tumor microenvironment, single-cell transcriptome analysis, Nx1-seq

## 1. Introduction

Tumor tissues are aggregates of various cell populations, and each single cell or cell population plays an important role for cancer progression and regression. The representative cell populations of the tumor microenvironment are cancer cells, surrounding normal cells, and infiltrated immune cells of all types. Anticancer agents and immune checkpoint blockers, such as programmed death receptor-1 (PD-1) and its ligand, have been widely used in patients, and the curative effect is great. However, for many patients, these treatments are ineffective because the minor cell populations escape the immune system. Therefore, a deeper understanding of the tumor microenvironment immunology will be critical for immunotherapy to become a standard therapy. In addition, it is important to clarify patient and tumor-dependent cell phenotypes by gene expression analysis because the composition and functions of the tumor microenvironment are heterogeneous between cancers and patients.

Previous gene expression measurements have been performed on bulk samples. Conventional bulk-based RNA sequencing or microarrays alone or in combination with flow cytometry can provide a full view of all gene expression, and it is useful to

investigate the tumor microenvironment. However, a blended gene expression analysis might mask the minor cell population, which may be the origin of tumor progression. To overcome this problem, RNA sequencing methods that can analyze mRNA expression at the single-cell level from thousands of individual cells are required. The fundamentally necessary approaches of single-cell RNA sequencing are: (1) single-cell isolation with a high survival rate, (2) cell lysis to obtain mRNA, (3) conversion of mRNA into cDNA, (4) specific amplification of cDNA, (5) cDNA fragmentation process, and (6) creation of high-quality sequencing libraries. After single-cell isolation, there are some innovative single-cell transcriptome analysis methods (e.g., CEL-seq [1], Quartz-seq [2], Quartz-seq2 [3], Smart-seq [4], Drop-seq [5], iDrop RNA sequencing [6], Cyto-Seq [7], automated microwell-based RNA sequencing [8], and our next generation 1-cell sequencing; Nx1-seq [9]), and every method uses oligo-dT primers containing cell-specific bar-codes, which tag cDNA from single cells.

Although cell number, tissue volume analyzed, analysis sensitivity, and overall cost for creating libraries are completely different, any methods with an efficient data analysis procedure would be particularly useful to understand cellular heterogeneity and to identify rare cell populations. For example, six prominent single-cell RNA sequencing methods: CEL-seq2, Drop-seq, MARS-seq, SCRB-seq, Smart-seq, and Smart-seq2 have been compared in mouse embryonic stem cells [10]. If single-cell transcriptome analysis were performed in a limited number of cells or small tissue volume, SCRB-seq and MARS-seq will have better sensitivity. Yet, Smart-seq2 may detect the highest number of genes per cell with amplification noise. Drop-seq is a preferable and more cost-effective method for large numbers of cells with low sequencing depth. In terms of the number of reads per cell and genes, we also compared our Nx1-seq and Drop-seq, and it revealed similar sensitivity [9]. Recently, another microwell-based RNA sequencing has been developed [11], and this is a simple, high-throughput, and low-cost device. The principle of their device is similar to Cyto-Seq and Nx1-seq, but the differences are the beads material and the loading order of single cells and beads to the microwell. They have attempted to construct a “mouse cell atlas” by using over 50 mouse tissues, organs, and cell cultures. One of the reasons they can analyze a large sample amount is the low-cost device without any expensive, exclusive apparatus and kits for capturing mRNA from a single cell. Previously, a detailed description of each method was thoroughly reviewed [12]; yet, innovative new technologies for single-cell RNA sequencing are still to be developed. We also continue improving our Nx1-seq device progressively.

## 2. Single-cell transcriptome analysis for cancer tissues

To find new molecular targets for a cancer prognosis prediction method, it requires an understanding of the single-cell level transcriptome heterogeneity in tumor tissues and their microenvironment. Bulk-based RNA sequencing may also contribute to development of new minimally invasive monitoring of circulating tumor cells or cancer gene-transferred macrophages and lymphoid cells. If the targeted cancer antigen and/or cell surface protein were held in small cell populations, the intensity signal of the gene expression would be weak. In this case, single cell transcriptome analysis is a useful tool to identify the small cell population and obtain all of the gene information in this population. In the next chapter, we describe our Nx1-seq methods in detail and show a representative Nx1-seq application in human endometrioid adenocarcinoma tissue. At this time, there are no reports about single-cell transcriptome analysis for endometrioid adenocarcinoma, except our research [9]. Here, we briefly summarize recent applications of single-cell RNA sequencing in one of the major gynecological cancers, breast cancer.

Chung et al. conducted single-cell transcriptome analysis for 11 primary tumors and 2 metastatic lymph nodes from 11 patients, representing 4 breast cancer subtypes [13]. It clearly displayed the carcinoma and tumor-infiltrating immune cells population using the 10–17  $\mu\text{m}$  integrated fluidic circuit mRNA sequencing chip in the  $C_1^{\text{TM}}$  Single-Cell Auto Prep System of Fluidigm®. The  $C_1^{\text{TM}}$  integrate fluidic circuit is an integrated microfluidic system that can automatically isolate individual cells from suspended cells. Subsequently, cell lysis buffer is automatically applied to individual cells to capture mRNA. It takes 5 h to make sequence-ready libraries from isolated cells, and the operation is simple [14]. The authors demonstrated that many T cells with high cytokine and chemokine expression were observed in three triple negative breast cancers (TNBC), and their phenotypes were regulatory T cells (two out of three patients) and another one was exhaustion and cytotoxicity signatures [13]. This result indicates that immune checkpoint blockers may be effective in the patient.

Recently, single-cell transcriptome analysis using 10X Genomics Chromium was reported in breast cancer [15, 16]. Cazet et al. investigated the anti-tumor inhibitor effects in a mouse tumor model, in terms of changes in the gene expression profiles of each cell population [15]. Tumor development and progression were associated with stiffness of the extracellular matrix, and collagen density in the tumor-stromal interface was reduced by small molecule inhibitor of smoothened (SMO) treatment. They also showed that the chemotherapy significantly slowed tumor growth and reduced the frequency of metastatic disease in xenograft models of human TNBC. In another article, an infiltrating T cell population in breast cancer was classified from 123 patients, and it demonstrated the importance of qualitative identification of  $\text{CD8}^+$  T cell subtypes [16].  $\text{CD8}^+ \text{CD103}^+$  T cells contained features of read tissue-resident memory, including high granzyme B, PD-1, and cytotoxic T lymphocyte (associated) antigen 4 (CTLA-4), rather than  $\text{CD8}^+ \text{CD103}^-$  T cells, meaning that these are target cells for immune checkpoint blockers.

The above representative reports using single-cell read transcriptome analysis were well analyzed, but we speculate that the cost for creating a sequence library per sample using commercially available device-dependent kits may be expensive. Many samples should be analyzed in a clinical study because the observed microenvironment heterogeneity is patient-, malignant-, or organ-dependent. In addition, if characterization of tumor gene expression profiling was recognized according to the individual's region or country, it should be performed locally because fresh samples, not frozen ones, are better to analyze for RNA sequencing. From this standpoint, a device with low-cost, in high sensitivity, and easy performance is recommended.

### 3. Nx1-seq

The major component of Nx1-seq (next generation 1-cell sequencing) consists of bar-code beads and a specifically processed microwell. In this chapter, we describe these devices in further detail.

#### 3.1 Bar-code beads

Oligonucleotides on beads have the following sequence: (1) “root array” is used as a priming site for subsequent PCR; (2) “cell bar-code” allocates 12 bp of oligonucleotide to identify cells, and the bar-code has  $4^{12} = 16,777,216$  various patterns; (3) “UMI” (a unique molecular identifier) has 8 bp of oligonucleotide to



eliminate gene duplication bias and improve signal/noise ratio by PCR, meaning that 1-cell bar-code has 1 UMI; and (4) “poly-dT” array consists of 25 bp oligo dT sequences for capturing polyadenylated mRNA. The bar-code beads (“root”-“cell bar-code”-“UMI”-“poly-dT”) were made by following a modified instruction manual for the GS Junior Titanium emulsion PCR Kit (Lib-L) from Roche® Applied Science or synthesized by ChemGenes Corporation (Wilmington, MA, USA) with additional annealing and ligation of the poly-dT array in our laboratory. The detailed method for generating bar-code beads using the emulsion PCR kit is described in our previous report [9]. We could get randomly synthesized various “cell bar-code” inserted bar-code beads, and the beads were washed with Low TE buffer (10 mM Tris-HCl pH 8.0, 0.1 mM EDTA pH 8.0) and stored at  $-20^{\circ}\text{C}$  until use.

3.2 Microwell slide

The microwell plate was prepared using polydimethylsiloxane (PDMS) and was cut  $2 \times 2 \times 2 \text{ cm}$  using cutting dies (Noda Co. Ltd., Osaka, Japan) which contained  $1.3\text{--}1.6 \times 10^5$  microwells. The size of one microwell was  $25 \pm 3 \mu\text{m}$  diameter,  $40 \pm 8 \mu\text{m}$  height,  $20 \pm 9 \mu\text{L}$  capacity (column-shape), and the distance between microwells was  $5 \mu\text{m}$  (YODAKA CO., Ltd., Kanagawa, Japan). If the size of the target cell was not between 15 and  $25 \mu\text{m}$ , the diameter and height sizes were easily adjusted. The PDMS microwell plate was placed in an oxygen plasma chamber for hydrophilic processing because PDMS is a hydrophobic material. The microwell plate was quickly set into the Nunc™ Lab-Tek™ Chamber slide system (Thermo Fisher Scientific, Waltham, MA, USA), and bar-code beads were applied to the microwell plate. If the expected number of cells obtained from the tumor tissue was  $<1 \times 10^5$  cells, the PDMS microwell was cut  $\sim 1/4$  or  $1/2$  of its size and set into the appropriate Nunc™ Lab-Tek™ Chamber slide system (**Figure 1**). The PDMS microwell plate was kept at  $4^{\circ}\text{C}$ , meaning that the Nx1-seq device can be stored until use.

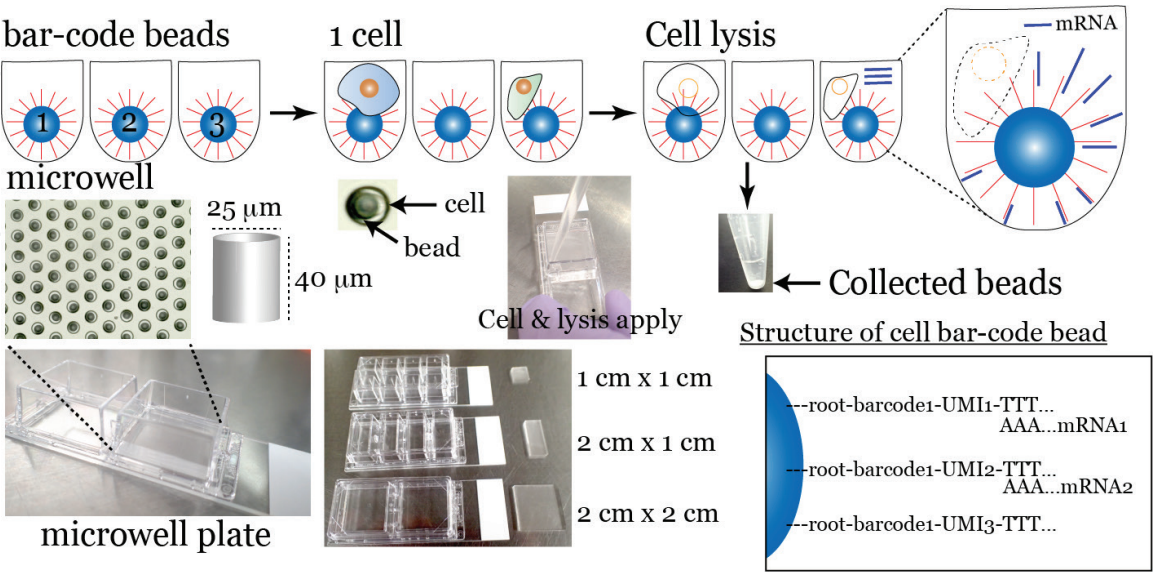


**Figure 1.** Schematic drawings of Nx1-seq. Cell bar-code beads (see the structure of cell bar-code bead) were filled into microwells, and an adequate number of single cells was applied. Cells were dissolved in lysis buffer, and mRNA from the cell was captured by cell bar-code beads in each microwell. After cellular lysis, all beads were collected into a single tube. Images of the microwell plate show that our device had some variations for differences of the number of applied cells.

### 3.3 Lysis of cells

After single cell isolation,  $\sim 1-2 \times 10^5$  cells mixed with 3.7 mL of cold PBS were applied to PDMS microwell plate ( $2 \times 2 \times 2$  cm) and put the cover without entering a bubble. The microwell plate was put on ice for 10–15 min, which let the cells settle into the microwell by gravity. About 5% of whole microwells were filled with single cells according to Poisson distribution. The solution was removed from the microwell plate, and 1 mL of fresh cold PBS was gently applied. The washing process was repeated by 3–4 times. The reagent composition of 1 mL of cell lysis buffer was; 2 mg of *N*-Lauroylsarcosine sodium salt, 200  $\mu$ L of 1 M Tris-HCl pH 7.5, 40  $\mu$ L of 0.5 M EDTA pH 8.0, 750  $\mu$ L of deionized water, 50  $\mu$ L of 1 M dithiothreitol solution. The microwell plate was put on a microscopy, and we found the microwell which contains only cell without bar-code bead, then PBS was removed and 1 mL of cell lysis buffer was gently applied from the corner of the microwell. Most cells were getting to dissolve within 1–3 min, but it kept for 8 min. The cell lysis buffer was removed carefully and washing buffer (200 mM Tris-HCl pH 7.5, 20 mM EDTA, 50 mM DTT, 0.2% *N*-Lauroylsarcosine sodium salt, 2% Ficoll) was added. Conversion of mRNA into cDNA was done by SuperScript™ II or IV Reverse Transcriptase (Thermo Fisher Scientific).

## 4. Nx1-seq application to human endometrioid adenocarcinoma tissues

Previously, we reported the application of Nx1-seq to human endometrioid adenocarcinoma (EA) tissues [9]. Here, we summarize the result shortly. EA tissues were removed from the myometrial infiltration side (M-side) and endometrial side (E-side). Myometrial invasion is an independent prognostic parameter of EA, and invasion is correlated with the risk of metastasis to the lymph nodes. Single-cell analysis in each side revealed that EA had six cancer (cluster #0, 1, 2, 3, 5, 6), two macrophage (#4, 8), and one T cell population (#7) (**Figure 2A**). To analyze the sequencing data, we used Seurat software (<http://satijalab.org/seurat/>), which is an open tool for analyzing single-cell genomics in R (<http://www.R-project.org/>). As shown in **Figure 2B**, the distribution of cancer cells on the E-side and M-side differed, and the majority of the macrophage cluster (#4) was on the M-side. The number of infiltrating macrophages was not different between sides (**Figure 2C**), but macrophage specificity was more cytotoxic T lymphocytes (CTL)-like on the M-side. Macrophages on the M-side had higher expression of inflammatory chemokines, C-X-C motif chemokine ligand 3 and 8 (*CXCL3* and *CXCL8*) and NF- $\kappa$ -B inhibitor $\alpha$  (*NFKBIA*) (**Figure 2D**). The proportion of macrophages expressing the inflammatory factors *CCL5*, *IL10* and *IL6* did not differ among the two sides (data not shown). It has been widely believed that many cells expressing some malignancy-related genes exist on the M-side; however, our previous result showed that cancer cells on the E-side were highly malignant when compared to those on the M-side.

In addition, a cancer stem-like cell population was also higher on the E-side (e.g., the ratio of *SOX2*<sup>+</sup> cells on E-side vs. M-side was 17 vs. 6%, respectively) [9]. These data reveal that cells with high malignant potential (HMP) are present at the same site of cancer tissue (E-side) in EA. To confirm our hypothesis, we focused on the ubiquitin C-terminal hydrolase L1 (*UCHL1*) gene. Protein ubiquitination or de-ubiquitination regulates cell growth, differentiation, transcription, and tumor prognosis. The function of *UCHL1* in neurodegenerative disorders, particularly in Alzheimer's disease and Parkinson's disease has been reported, and decreased

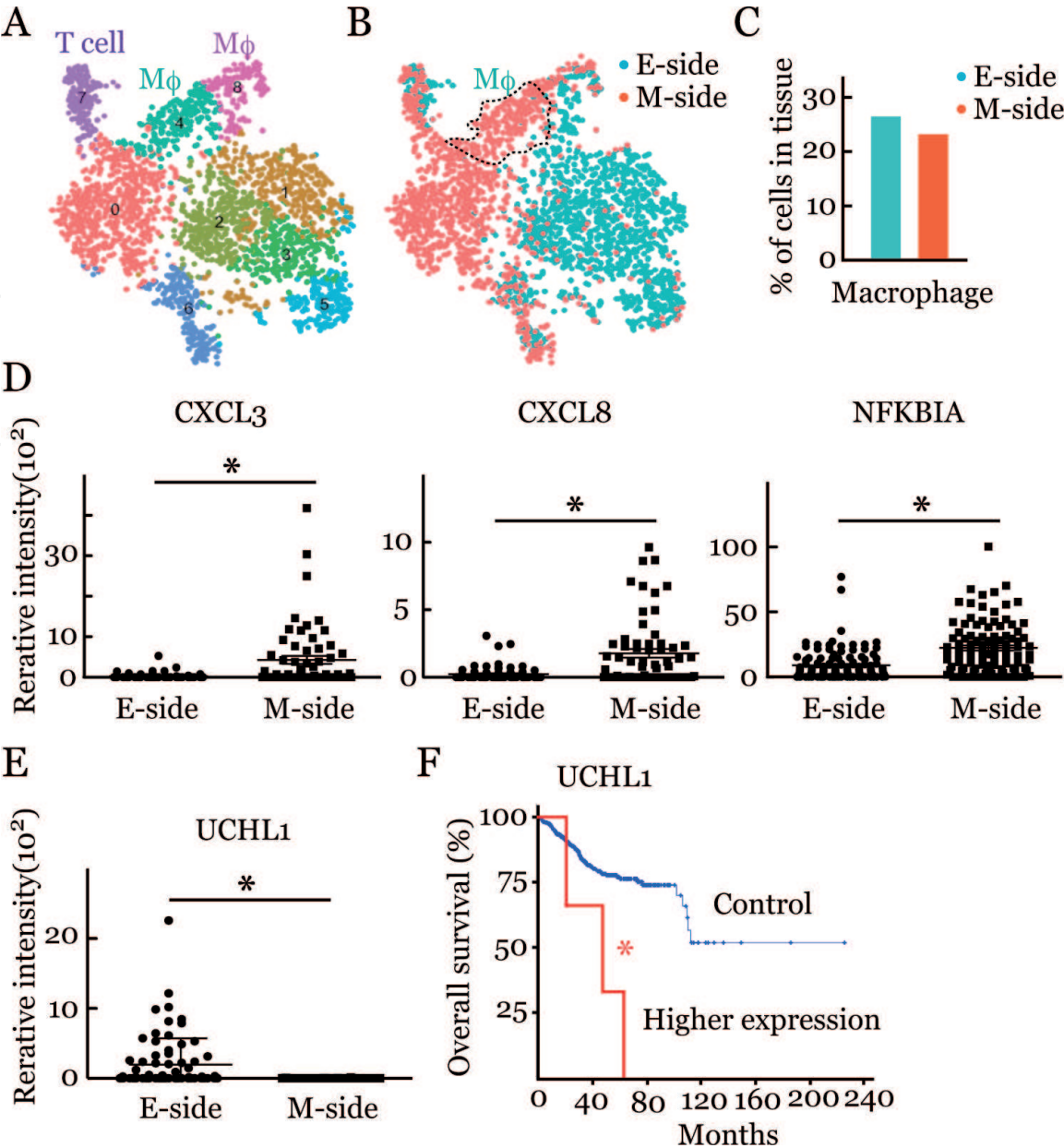


**Figure 2.** Clustering of human endometrioid adenocarcinoma tissue. (A) Nine clusters were identified by t-SNE analysis. (B) Cluster analysis in each side; sky blue dots indicate the endometrial side (E-side) and red dots are the myometrial infiltration side (M-side). (C) The ratio (%) of macrophages in the E- or M-side of tissues is shown. (D) Relative intensity of CXCL3, CXCL8, and NFKBIA in both sides. \* $p < 0.001$  for E-side vs. M-side by the Mann-Whitney U-test. (E) Summary of UCHL1 expression. Relative intensity of UCHL1 is shown, and \* $p < 0.001$  for E-side vs. M-side by the Mann-Whitney U-test. (F) Overall survival of Kaplan-Meier estimate was obtained from cBioPortal for CANCER GENOMICS. Blue: control, Red: relatively higher expression group. \* $p < 0.001$  for the control vs. high UCHL1 expression.

hydrolase activity and UCHL1 ligase activity may affect the neurodegeneration [17, 18]. In our EA tissue, the relative intensity of UCHL1 expression was higher on the E-side (Figure 2E). The functional role of UCHL1 in human tumor malignancy is still unresolved, but this gene has been reported to be cancer-related in endometrial cancer patients [19]. Goto et al. demonstrated that activation of UCHL1 via hypoxia inducible factor-1 (HIF-1) is the key regulator for underlying mechanism of tumor metastasis, and they expected UCHL1 as prognostic marker and treatment target for breast and lung cancers [20].

From the enormous single-cell RNA-sequencing data, the researcher must determine to manage and understand the functional meaning of the cell population. In particular, understanding how the gene is related to overall survival of EA patients in the clinical site is useful. Hence, we used the “cBioPortal For CANCER



GENOMICS” website and chose “Uterine Corpus Endometrial Carcinoma (EC) (TCGA, Provisional).” Subsequently, we set “Genomic profiles” as “mRNA Expression,” and chose “mRNA Expression z-Score (microarray),” then input the gene name “*UCHL1*” (<http://www.cbioportal.org/>). Overall Survival of Kaplan-Meier (K-M) Estimate showed that high *UCHL1* expression in endometrial carcinoma patients significantly decreased survival time (**Figure 2F**). The median months survival in the *UCHL1* high group was 48.75 months. The log-rank *p* value for K-M analysis for correlation between mRNA expression level and patient survival was  $1.965 \times 10^{-4}$ . The Overall Survival of K-M Estimate was not calculated from the EA but EC dataset, however EA of the endometrium is the most common type of EC [21]. Therefore, the result indicates that higher expression of *UCHL1* on the E-side somehow affects EA progression, and it supports our hypothesis that cells with HMP are present on the E-side. Whether we chose other data set “Uterine Corpus Endometrial Carcinoma (TCGA, Nature 2013),” the result of Overall Survival of K-M Estimate was also significant ( $p = 1.06 \times 10^{-3}$ ). The median months of disease-free in high *UCHL1* patients was 12.94 months, and it was significantly earlier by the Disease/Progression-free Kaplan-Meier Estimate. However, the significant correlation was not observed if we chose “mRNA Expression z-Scores (RNA Seq V2 RSEM), z-score threshold  $\pm 2.0$ ” ( $p = 0.955$ ). There was other useful database to realize the overall survival of EC patients. We used the “THE HUMAN PROTEIN ATLAS” website and input the gene name “*UCHL1*,” then set “PATHOLOGY ATLAS” (<http://www.proteinatlas.org/>). The prognostic summary highlighted that *UCHL1* was the candidate as the prognostic marker in EC. The 5-year survival in the *UCHL1* high or low group was 66 or 86% respectively, and the *p* score was  $4.1 \times 10^{-5}$  from the total of 541 female patients.

As shown in **Figure 3**, there was significant differences about *UCHL1* expression between each side, and immunostaining of *UCHL1* showed a similar staining

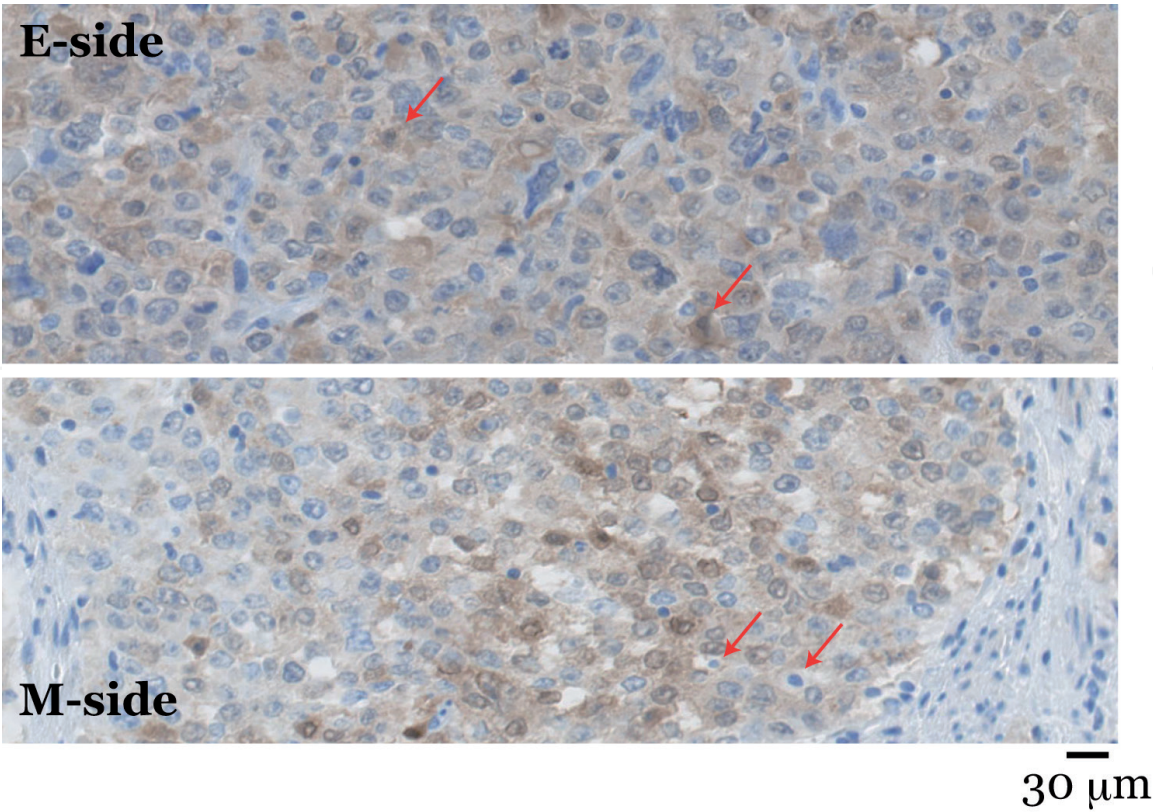


**Figure 3.**  
*Immunohistochemistry of UCHL1 in E-side and M-side. Macrophages identified by pathologist are also positively stained. Red arrows show macrophage. The scale bar indicates 30 μm.*



pattern in macrophages as well as cancer cells. Also, *UCHL1* staining in E-side was relatively higher. These data indicate that microenvironment of tumor tissue might affect the gene properties of immune cells, and gene expression pattern might resemble closely to cancer cells.

The high expression of *CXCL3* was not related to the prognosis of EA ( $p = 0.987$ ) by the CANCER GENOMICS, but *CXCL3* high group significantly improved 5-year overall survival by the PROTEIN ATLAS. At this moment, there was only one patient whose expression of *CXCL8* was high in the CANCER GENOMICS, but 5-year survival of *CXCL8* high or low group in EC patients was 79 or 70% respectively, and there was no significant difference. In contrast, higher expression of *NFKBIA* significantly decreased survival time by “mRNA Expression z-Score (microarray)” ( $p = 0.0246$ ), but not “mRNA Expression z-Score (RNA Seq V2 RSEM)” by the CANCER GENOMICS. In contrast, the 5-year overall survival in the PROTEIN ATLAS was not significant. These results indicate that the researcher must use some database to understand how the target genes are related to the prognosis of cancers. Further studies for other HMP-related genes are ongoing in our laboratory.

## 5. Conclusion

Single-cell sequencing is believed to be a powerful tool to answer unknown biological questions, and researchers may have many expectations to find new insights of their hypotheses. Indeed, bulk-based RNA sequencing is averaged across a cell population, but the method to obtain total RNA is relatively simple and easy. Most importantly, we can detect gene expression profiling of the whole tissue. Of course, as mentioned above, the existence of minor cell populations, such as cancer stem-like cells, may not be detected in bulk-based RNA sequencing data. If the researchers knew the biomarkers of targeted cells in small population, the gene can be detected from the bulk-based RNA sequencing data. But it is unknown which cell expresses and how many cells have the targeted gene because of the averaged data by bulk-based RNA sequencing. Thus, it is better to ponder over which method is aimed at the biological question before choosing more difficult and expensive single-cell RNA sequencing.

Current protocols of dispersing single cells in each tissue are not optimized worldwide; therefore, some cells or cell populations may disappear in the course of isolating single cells from tumor tissue. One of the most important procedures for single-cell RNA sequencing is isolation of single cells from tumor tissues. Mechanical and/or enzymatic cell distributed processes followed by fluorescence-activated cell sorting (FACS), magnetic-activated cell sorting (MACS), or density-gradient method are the current standard [22], but the softness or hardness of tissues differs depending on the tumor. Inappropriate single-cell isolation methods are biased; therefore, more detailed studies are needed to optimize isolation of single cells for each tissue.

Nonetheless, single-cell sequencing is a great tool for detecting heterogeneous subpopulations, cell-to-cell communication, and spatial interactions. Moreover, the many gene expression changes by carcinostatic agents can be monitored. To analyze extensively heterogeneous clinical samples, highly sensitive, low cost, quick, and simple technologies to capture mRNA from a single cell are required. Our newly developed single-cell transcriptome analysis, Nx1-seq, can be a useful tool to understand tumor microenvironments with high sensitivity and low cost. This new approach is a simple method, and it can be used to analyze several hundreds to tens of thousands of cells without specialized equipment. Further, it is easy to

change the size of the microwell for larger or smaller cells. Furthermore, microwells equipped with bar-code beads in the Nunc™ Lab-Tek™ Chamber slide system can be stored for several months before use. Nx1-seq is a powerful approach for characterizing cellular diversity under physiological and pathological conditions. The combined analysis of t-SNE by Seurat and detailed gene profiling can discover new tumor biomarkers or new target genes for regression of tumor tissues. We continue to develop better Nx1-seq devices to satisfy requests from researchers. It is about continued learning on a daily basis.

## Acknowledgements

The authors would like to thank Y. Kamide, S. Kurokawa, and H. Sekine for technical assistance with the experiments. We also thank A. Tagata for assistance of accounting work. We greatly appreciate Dr. Y. Takamura for supplying PDMS membrane. Prof. T. Torigoe and Dr. Y. Hirohashi gave us the data of UCHL1 immunohistochemistry and constructive comments, thank you. This work is supported by the Japan Agency for Medical Research and Development (AMED). We would like to thank Editage (<http://www.editage.jp>) for English language editing.

## Conflict of interest

The authors have no conflicts of interest directly relevant to the content of this article.

## Author details

Sadahiro Iwabuchi\* and Shinichi Hashimoto  
Department of Integrative Medicine for Longevity, Graduate School of Medical Sciences, Kanazawa University, Kanazawa, Ishikawa, Japan

\*Address all correspondence to: [s\\_iwabuchi@staff.kanazawa-u.ac.jp](mailto:s_iwabuchi@staff.kanazawa-u.ac.jp)

## IntechOpen

© 2019 The Author(s). Licensee IntechOpen. This chapter is distributed under the terms of the Creative Commons Attribution License (<http://creativecommons.org/licenses/by/3.0>), which permits unrestricted use, distribution, and reproduction in any medium, provided the original work is properly cited. 

## References

- [1] Hashimshony T, Wagner F, Sher N, Yanai I. CEL-seq: Single-cell RNA-Seq by multiplexed linear amplification. *Cell Reports*. 2012;2:666-673. DOI: 10.1016/j.celrep.2012.08.003
- [2] Sasagawa Y, Nikaido I, Hayashi T, Danno H, Uno KD, Imai T, et al. Quartz-Seq: A highly reproducible and sensitive single-cell RNA sequencing method, reveals non-genetic gene-expression heterogeneity. *Genome Biology*. 2013;14:R31-47. DOI: 10.1186/gb-2013-14-4-r31
- [3] Sasagawa Y, Danno H, Takada H, Ebisawa M, Tanaka K, Hayashi T, et al. Quartz-Seq2: A high-throughput single-cell RNA-sequencing method that effectively uses limited sequence reads. *Genome Biology*. 2018;19:29-52. DOI: 10.1186/s13059-018-1407-3
- [4] Picelli S, Faridani OR, Bjroklund AK, Winberg G, Sagasser S, Sandberg R. Full-length RNA-seq from single cells using Smart-seq2. *Nature Protocols*. 2014;9:171-181. DOI: 10.1038/nprot.2014.006
- [5] Macosko EZ, Basu A, Satija R, Nemesh J, Shekhar K, Goldman M, et al. Highly parallel genome-wide expression profiling of individual cells using nanoliter droplets. *Cell*. 2015;161:1202-1214. DOI: 10.1016/j.cell.2015.05.002
- [6] Klein AM, Mazutis L, Akartuna L, Tallapragada N, Veres A, Li V, et al. Droplet barcoding for single cell transcriptomic applied to embryonic stem cells. *Cell*. 2015;161:1187-1201. DOI: 10.106/j.cell.2015.04.044
- [7] Fan X, Zhang X, Wu X, Guo H, Hu Y, Tang F, et al. Single-cell RNA-seq transcriptome analysis of linear and circular RNAs in mouse preimplantation embryos. *Genome Biology*. 2015;16:148-164. DOI: 10.1186/s13059-015-0706-1
- [8] Yuan J, Sims PA. An automated microwell platform for large-scale single cell RNA-seq. *Scientific Reports*. 2016;6:33883-33892. DOI: 10.1038/srep33883
- [9] Hashimoto S, Tabuchi Y, Yurino H, Hirohashi Y, Deshimaru S, Asano T, et al. Comprehensive single-cell transcriptome analysis reveals heterogeneity in endometrioid adenocarcinoma tissues. *Scientific Reports*. 2017;27:14225-14238. DOI: 10.1038/s41598-017-14676-3
- [10] Ziegenhain C, Vieth B, Parekh S, Guillaumet AA, Smets M, Leonhardt H, et al. Comparative analysis of single-cell RNA sequencing methods. *Molecular Cell*. 2017;65:631-643. DOI: 10.1016/j.molcel.2017.01.023
- [11] Han X, Wang R, Zhou Y, Fei L, Sun H, Lai S, et al. Mapping the mouse cell atlas by microwell-seq. *Cell*. 2018;172:1091-1107. DOI: 10.1016/j.cell.2018.02.001
- [12] Simone P. Single-cell RNA-sequencing: The future of genome biology is now. *RNA Biology*. 2017;14:637-650. DOI: 10.1080/15476286.2016.1201618
- [13] Chung W, Eum HH, Lee HO, Lee KM, Lee HB, Lim KT, et al. Single-cell RNA-seq enables comprehensive tumour and immune cell profiling in primary breast cancer. *Nature Communications*. 2017;8:15081. DOI: 10.1038/ncomms15081
- [14] DeLaughter DM. The use of the Fluidigm C1 for RNA expression analyses of single cells. *Current Protocols in Molecular Biology*. 2018;122:e55. DOI: 10.1002/cpmb.56
- [15] Cazet AS, Hui MN, Elsworth BL, Wu SZ, Roden D, Chan CL, et al. Targeting stromal remodeling and



cancer stem cell plasticity overcomes chemoresistance in triple negative breast cancer. *Nature Communications*. 2018;**9**:2897-2904. DOI: 10.1038/s41467-018-05220-6

[22] Hu P, Zhang W, Xin H, Deng G. Single cell isolation and analysis. *Frontiers in Cell and Development Biology*. 2016;**4**:116-127. DOI: 10.3389/fcell.2016.00116

[16] Savas P, Virassamy B, Ye C, Salim A, Mintoff CP, Caramia F, et al. Single-cell profiling of breast cancer T cells reveals a tissue-resident memory subset associated with improved prognosis. *Nature Medicine*. 2018;**24**:986-993. DOI: 10.1038/s41591-018-0078-7

[17] Liu Y, Fallon L, Lashuel HA, Lansbury PT Jr. The UCH-L1 gene encodes two opposing enzymatic activities that affect alpha-synuclein degradation and Parkinson's disease susceptibility. *Cell*. 2002;**111**:209-218. DOI: 10.1016/S0092-8674(02)01012-7

[18] Choi J, Al L, Weintraub ST, Rees HD, Gearing M, Chin LS, et al. Oxidative modifications and down-regulation of ubiquitin carboxyl-terminal hydrolase L1 associated with idiopathic Parkinson's and Alzheimer's diseases. *The Journal of Biological Chemistry*. 2004;**279**:13256-13264. DOI: 10.1074/jbc.M314124200

[19] Nakao K, Hirakawa T, Suwa H, Kogure K, Ikeda S, Yamashita S, et al. High expression of ubiquitin C-terminal hydrolase L1 is associated with poor prognosis in endometrial cancer patients. *International Journal of Gynecological Cancer*. 2018;**28**:675-683. DOI: 10.1097/IGC.0000000000001201

[20] Goto Y, Zeng L, Yeom CH, Zhu Y, Morinibu A, Shinomiya K, et al. UCHL1 provides diagnostic and antimetastatic strategies due to its deubiquitinating effect on HIF-1 $\alpha$ . *Nature Communications*. 2015;**6**:6153-6165. DOI: 10.1038/ncomms7153

[21] Morice P, Leary A, Creutzberg C, Abu-Rustum N, Darai E. Endometrial cancer. *Lancet*. 2016;**387**:1094-1108. DOI: 10.1016/S0140-6736(15)00130-0